



**The Origin of Oltu Stone (Turbostratic Carbon) from the Olur-Tortum Area:  
A Natural Composite Carbonaceous Material (Erzurum, Türkiye)**  
*Olur-Tortum Bölgesindeki Oltu Taşının (Turbostratik Karbon) Kökeni:  
Karbonlu Doğal Bir Kompozit Malzeme, Erzurum, Türkiye*

**Cahit Helvacı<sup>1,\*</sup>, Murat Hatipoğlu<sup>2</sup>, Daniele Passeri<sup>3</sup>, Neşat Konak<sup>4</sup>,  
Eyyüp Hikmet Kınacı<sup>5</sup>**

<sup>1</sup>Dokuz Eylül University, Faculty of Engineering, Department of Geological Engineering TR-35370  
Buca-İzmir/Türkiye

<sup>2</sup>Dokuz Eylül University, The Graduate School of Natural and Applied Sciences, Department of Natural Building  
Stones and Gem Stones TR-35370 Buca-İzmir/ Türkiye

<sup>3</sup>University of Rome, Department of Fundamental and Applied Sciences for Engineering I-00161 Rome/ITALY

<sup>4</sup>MTA General Directorate of Mineral Research and Exploration, Department of Geological Research,  
TR-06800 Ankara/Türkiye

<sup>5</sup>Batman University, Technical Sciences Vocational School, Handicrafts Department, TR-72060 Batman/Türkiye

• Geliş/Received: 29.05.2024

• Düzeltilmiş Metin Geliş/Revised Manuscript Received: 12.07.2024

• Kabul/Accepted: 12.07.2024

• Çevrimiçi Yayın/Available online: 26.11.2024

• Baskı/Printed: 31.05.2025

*Araştırma Makalesi/Research Article*

*Türkiye Jeol. Bül. / Geol. Bull. Turkey*

**Abstract:** This study focuses on geological, microstructural, oxygen isotopic, and thermogravimetric investigations of Oltu stone, which is the most important turbostratic carbonaceous material in Turkey.

The results of our investigations indicate that the carbonaceous Oltu stone material (specific gravity of 1.317) is not an organic material, such as jet, derived from fossilized wood. Rather, it is composed of a carbonaceous phase intermediate between amorphous carbon and crystallized graphite (termed turbostratic carbon), that is intercalated with flysch and formed by the reduction of seeping magmatic carbon dioxide during the diagenesis of Upper Jurassic-Lower Cretaceous marine sediments. Oxygen isotope analyses (SMOW) (using EA-IRMS) of both Oltu stone ( $\delta^{18}\text{O} = +37.2\text{‰}$  to  $+40.8\text{‰}$ ) and the enclosing flysches ( $\delta^{18}\text{O} = +10.3\text{‰}$  to  $+12.3\text{‰}$ ) suggest that the nodules formed during diagenesis at a temperature of around 50 °C. However, they are enclosed in flysches whose grains are derived from rocks that formed at significantly higher temperatures, perhaps above 100 °C.

The main industrial use of Oltu stone is as host material for diamond coating, as the  $\text{sp}^3$  bonds in the material can provide nucleation sites for diamond crystals and improve the nucleation rate at the early stage of diamond deposition on turbostratic carbon.

**Keywords:** Erzurum, Olur-Tortum geological zone, Oltu stone, Turbostratic carbon, Turkey.

**Öz:** Bu çalışma, Türkiye'nin en önemli turbostratik karbonlu malzemesi olan Oltu-taşının jeolojik, mikroyapısal, oksijen izotopik ve termogravimetrik incelemelerine odaklanmaktadır.

Bu çalışmada elde edilen veriler, karbonlu Oltu taşı malzemesinin (özgül ağırlığı 1,317) karakehribar gibi fosilleşmiş ağaçtan türetilmiş organik bir malzeme olmadığını göstermektedir. Daha ziyade, Üst Jura-Alt Kretase denizel çökellerinin diyajenezi sırasında yukarı doğru sızan magmatik karbondioksitin indirgenmesi sonucu oluşan

ve fişlerle arakatkılı olan amorf karbon ile kristalize grafit (turbostratik karbon olarak adlandırılır) arasında bir karbonlu fazdan oluşmaktadır. Hem Oltu taşının ( $\delta^{18}\text{O} = +37,2\text{‰}$  ila  $+40,8\text{‰}$ ) hem de onu çevreleyen fişlerin ( $\delta^{18}\text{O} = +10,3\text{‰}$  ila  $+12,3\text{‰}$ ) oksijen izotop analizleri (SMOW) (EA-IRMS kullanılarak), nodüllerin diyajenez sırasında yaklaşık  $50\text{°C}$  sıcaklıkta oluştuğunu, ancak taneleri önemli ölçüde daha yüksek bir sıcaklıkta, belki de  $100\text{°C}$ 'nin üzerinde oluşan kayalardan gelen fişlerle ile çevrelendiğini göstermektedir.

Oltu-taşının başlıca endüstriyel kullanımı, elmas kaplamada kullanılan bir malzeme olmasıdır, çünkü malzemedeki  $\text{sp}^3$  bağları elmas kristalleri için çekirdeklenme alanları sağlayabilir ve turbostratik karbon üzerine elmas biriktirmenin erken aşamasında çekirdeklenme oranını artırabilir.

**Anahtar Kelimeler:** Erzurum, Olur-Tortum jeolojik alanı, Oltu taşı, Turbostratik karbon, Türkiye.

## INTRODUCTION

The toughness, durability, specific gravity, and colour of carbonaceous compact black material from different parts of the world (e.g. Turkey, Georgia, and Armenia) are highly variable due to different genetic and depositional conditions. However, those from the Oltu-Erzurum region in Turkey are characteristic and possibly unique. The material, which was shown to be a type of natural carbon black (Hatipoğlu et al., 2012), has some unusual physical characteristics and is referred to as turbostratic carbon. Subtle differences between carbon blacks can be attributed to their origin (Lahaye and Prado, 1981; Wang and Wolff, 1993; Donnet, 1994; Ungar et al., 2002; Ungar et al., 2005). Although carbon blacks are commonly used as filler in rubber production to modify the mechanical properties of the tire (Donnet, 1994; Clague et al., 1999; Hjelm et al., 2000), the internal structure of carbon black aggregates is not yet well understood. Graphite-like, quasi-crystalline domains, in which basal planes are parallel but angularly distorted and the interlayer spacing is different from that of pure graphite, were detected in carbon black particles, making them intermediate between crystalline and amorphous materials (Donnet, 1994).

In Turkey, a natural compact carbonaceous black material, which is traditionally known as “Oltu stone”, has been easily carved into gem objects for the jewellery market in the Oltu-Erzurum region (northeastern Anatolia) since the 18th century. Oltu stone is mainly used to make

ornaments such as rings, earrings, necklaces, bracelets, tiepins, pipes, studs, cigarette holders, and prayer beads—generally in combination with silver (Zengin, 1956; Çiftçi et al., 2002; Karayığit et al., 2002; Çiftçi et al., 2004; Karayığit, 2007; Hatipoğlu et al., 2012; Kalkan et al., 2012; Kınacı, 2013). The total potential reserve of Oltu stone in the study area is estimated to be approximately 150,000 tonnes.

In the last three decades, many studies were carried out about carbon blacks or turbostratic carbons using various methods (Bansal and Donnet, 1993; Gruber et al., 1993; Wang and Wolff, 1993; Donnet, 1994; Jawhari et al., 1995; Bertrand and Weng, 1999; Hjelm et al., 2000; Zerda et al., 2000; Lin, 2002; Probst and Grivei, 2002) so as to better determine chemical and physical properties and also to distinguish between those with organic origin, such as jet or carbon-like materials, in archaeological and gemmological science and those with inorganic origin not specifically derived from fossil hydrocarbons (Hunter et al., 1993; Gruber et al., 1994; Hatipoğlu et al., 2012). Carbon black surfaces and bulk structures of carbon black were studied by different methodologies, such as X-ray diffraction, neutron scattering (Franklin, 1950; Clague et al., 1999; Hjelm et al., 2000), Raman spectroscopy (Gruber et al., 1993 and 1994; Jawhari et al., 1995; Hatipoğlu et al., 2012; Hauptman et al., 2012), time-of-flight secondary ion mass spectrometry (TOF-SIMS), and X-ray photoelectron spectroscopy (XPS) (Bertrand and Weng, 1999). These studies provided a model

of carbon black microscopic aggregates that is widely accepted today. Specifically, carbon black is a material composed essentially of elemental carbon in the form of quasi-spherical particles that are fused together to form aggregates (Donnet, 1994; Clague et al., 1999).

The presence of two different carbon structures on carbon black surfaces, except for some mineral inclusions, was observed by X-Ray diffraction (Franklin, 1950, Donnet, 1994), and Raman spectroscopy (Gruber et al., 1993 and 1994; Jawhari et al., 1995; Zerda et al., 2000; Ungar et al., 2005; Hatipoğlu et al., 2012 and 2014). One of these has a structure like graphite and the second has an incompletely characterized amorphous carbon structure.

In the past, some scientific and promotional papers published on Oltu stone from the Erzurum region (Turkey) have mistakenly referred to this material as jet or jet-coal (Zengin, 1956; Çiftçi et al., 2002; Çiftçi et al., 2004; Karayığit et al., 2002; Karayığit, 2007; Kalkan et al., 2012, Toprak, 2013). Hunter et al. (1993) reported on the characterization of jet and similar materials using various physico-chemical techniques, including Raman spectroscopy. They found that the spectra of different materials (jet, lignite and cannel coal) did not exhibit significant differences. However, Smith and Clark (2004) noted, in an important review on the use of Raman microscopy in archaeological science, that the work of Hunter et al. (1993) was undertaken before highly sensitive Raman instruments became available.

In this study, we propose to establish some essential fingerprints for Oltu stone as natural turbostratic carbon that can be used to confirm its identity and geographical provenance. Natural turbostratic carbon has been an important material for industrial use in the world for several decades due to the coexistence of  $sp^3$  and  $sp^2$  bonds in turbostratic carbon materials. The  $sp^3$  bonds in turbostratic carbon provide nucleation sites for

diamond crystals and improve the nucleation rate at the early stage of deposition of diamond on turbostratic carbon. It is therefore highly likely that this material will be used for synthetic diamond production in the future.

## **MATERIAL and METHOD**

Chemical analyses, specific gravity measurements, X-ray diffraction patterns, scanning electron microscope images, atomic force microscope evaluations, differential thermal and thermogravimetric glow curves, oxygen isotope analyses, confocal micro-Raman bands, and Fourier-transform infrared graphic analyses were performed on Oltu stone to characterize this unusual homogeneous carbonaceous material and provide physical and mineralogical data relevant to its genesis. Detailed information about the composition of Oltu stone was obtained using a suite of techniques for whole rock analysis by the accredited ALS Chemex Laboratory in Canada. Carbon content was determined by combusting the sample in a Leco induction furnace and quantitatively detecting the carbon dioxide generated with infrared spectrometry. Sulphur content was measured with a Leco sulphur analyser with an infrared detection system. Minor elements were quantified by fusing the sample with lithium metaborate and lithium tetraborate and using inductively coupled plasma - atomic emission spectroscopy (ICP-AES). Trace elements were quantified by fusing the sample with lithium metaborate and using inductively coupled plasma - mass spectroscopy (ICP-MS). Loss on ignition was determined gravimetrically after heating a sample to 1000 °C for one hour. All the analyses were certified with the code number IZ11205067.

The specific gravity (SG) values of many Oltu stone samples were measured in this study using an electronic balance (measurement sensitivity of 0.001) with an SG kit, based on the formula ( $SG = \frac{W_{air}}{[W_{air} - W_{water}]}$ ). The test was performed in the

DGL-Gemmological Testing Laboratory at Dokuz Eylül University.

Crystalline components of the Oltu stone samples were detected using X-ray powder diffraction analysis with a Cubi-XRD device with a Cu tube and a graphic monochromator. The samples were analysed with Cu radiation and a 0.3 mm collimator at atmospheric pressure for 10 minutes each, in the range between  $5^\circ$  and  $70^\circ$  (2-theta). The d-spacing [Å] diffraction matching of the constituents obtained using the comparative matching technique is based on the positions of peaks with relative intensities  $[\% (I/I_0) > 1]$ , 2-theta values below  $70^\circ$ , and a tolerance range of  $\pm 0.01$ .

Internal structure of Oltu stone samples were observed at different magnifications up to 100,000x using a Philips XL 30S FEG (Field Transmission Gun) scanning electron microscope (SEM), after they were coated with a 5-nm-thick gold layer.

An atomic force microscope (AFM) device, the Nanosurf easyScan-2 (nanoscience Instruments) with 70-micron scanning range, was used to observe the surface morphologies of the representative Oltu stone samples. An AFM is a mechanical imaging instrument that measures the three-dimensional topography as well as the physical properties of a surface with a sharpened probe. In addition, the grain sizes of the samples were measured precisely. The precise particle sizes of any material can be measured because AFM does not use electromagnetic radiation, such as photon or electron beams, to create an image.

Analyses of stable oxygen isotopes made use of elemental-analysis-isotope-ratio mass spectrometry (EA-IRMS). Stable oxygen isotope data were obtained from 10 samples of Oltu stone materials and 5 samples of the enclosing flysch rocks.

Differential thermal analyses and thermogravimetric analyses (DTA/TGA) of the

Oltu-stone samples were conducted by using a thermal analysis system (Shimadzu TDG-60H). The DTA/TGA device was used to determine the changes in weight and heat-energy enthalpy against temperature in the samples. In the patterns, the change in DTA is in millivolts, and the change in TGA is in milligrams. Analyses were performed under a pure nitrogen atmosphere. The samples were approximately 6 mg in weight and were heated from room temperature (about  $25^\circ\text{C}$ ) up to  $1400^\circ\text{C}$  at a constant rate of  $10^\circ\text{C}/\text{min}$  to observe their heating behaviour. The drift of the mass gain observed in the TGA glow curves (the dotted red lines on the patterns) is a typical effect of buoyancy, so the mass gain is an experimental artefact exhibited by the thermobalance instrumentation. Therefore, the mass loss data obtained from the TGA curves were corrected to eliminate the buoyancy drift of the atmospheric gas. In fact, the only way to remove the effect of this buoyancy component is to decrease the heating rate and increase the sample mass. However, increasing the sample amount was not possible because of the small size of the sample crucible in the device used in the study. In addition, Oltu stone samples have some characteristic mineral inclusions. Therefore, the endotherms on the mass gain curves (the dotted blue lines on the patterns) of the DTA glow curves may also be an artefact due to the shift in baseline as the thermal mass of the specimen is reduced by the loss of carbonaceous material. Thus, the DTA curves were also corrected on the straight blue line as well as in the endotherm data.

Massive and unoriented samples of Oltu stone were placed on the stage of an Olympus BM-41 microscope, equipped with 10x and 50x objectives and part of a HORIBA Jobin Yvon Scientific XPLORE dispersive (visible) confocal micro-Raman spectrometer with a high throughput integrated spectrograph, which also includes a monochromator, a filter system and a charge-coupled device (CCD). Raman spectra were excited by a He-Ne laser (532 nm) at a resolution



of  $1 \text{ cm}^{-1}$  in the range between  $4000$  and  $50 \text{ cm}^{-1}$ . The micro-Raman analyses were performed on a dark background at room temperature. Repeated acquisitions using the highest magnification were accumulated to improve the signal-to-noise ratio. Spectra were calibrated using the  $520.5 \text{ cm}^{-1}$  line of a silicon wafer. As a baseline adjustment, spectral manipulation was carried out using the software supplied with the device. Spectrum acquisition details are as follows: objective, x50; filter, 100%; acquisitions averaged, 10; laser,  $532.06 \text{ nm}$ ; spectral window, auto; hole,  $500 \mu\text{m}$ ; slit,  $100 \mu\text{m}$ ; grating,  $1800 \text{ l/mm}$ ; ICS correction, on; and power,  $25 \text{ mW}$  at the sample.

## GEOLOGICAL SETTING OF THE STUDY AREA

Detailed field observations show that the northern Oltu region contains very complex geological

formations. This region, including the Oltu stone bearing deposits, is located in the northeastern Anatolian region between the Pontides belt (north Anatolian Mountain ranges) in the north and the Anatolide belt (inner Anatolian Mountain ranges) (Şengör et al., 1985; Koçyiğit et al., 1985).

Many geological sequences are superimposed along the NE-SW trending tectonic lines. Some of these sequences extend from the Jurassic to the Eocene. They are grouped into four zones in the Hopa-Şenkaya section based on different lithostratigraphic characteristics of the sequences. These zones, from NW to SW, are the Hopa-Borçka zone, the Artvin-Yusufeli zone, the Olur-Tortum zone, and the Erzurum-Kars ophiolite zone (Konak and Hakyemez, 2008) (Figures 1, 2, 3 and 4).



**Figure 1.** The Oltu-Erzurum region in Turkey where there are approximately 600 active and abandoned quarries for the carbon black material (Oltu stone). Oltu stone has been mined from the vicinity of Kırdağ Mountains in the Oltu region northeast of the city of Erzurum for about a century.

**Şekil 1.** Türkiye’de Oltu-Erzurum bölgesinde karbon siyahı malzemesi (Oltu taşı) için aktif ve terk edilmiş yaklaşık 600 taş ocağı bulunmaktadır. Oltu taşı, Erzurum şehrinin kuzeydoğusundaki Oltu bölgesinde bulunan Kırdağ Dağları civarından yaklaşık bir asırdır çıkarılmaktadır.

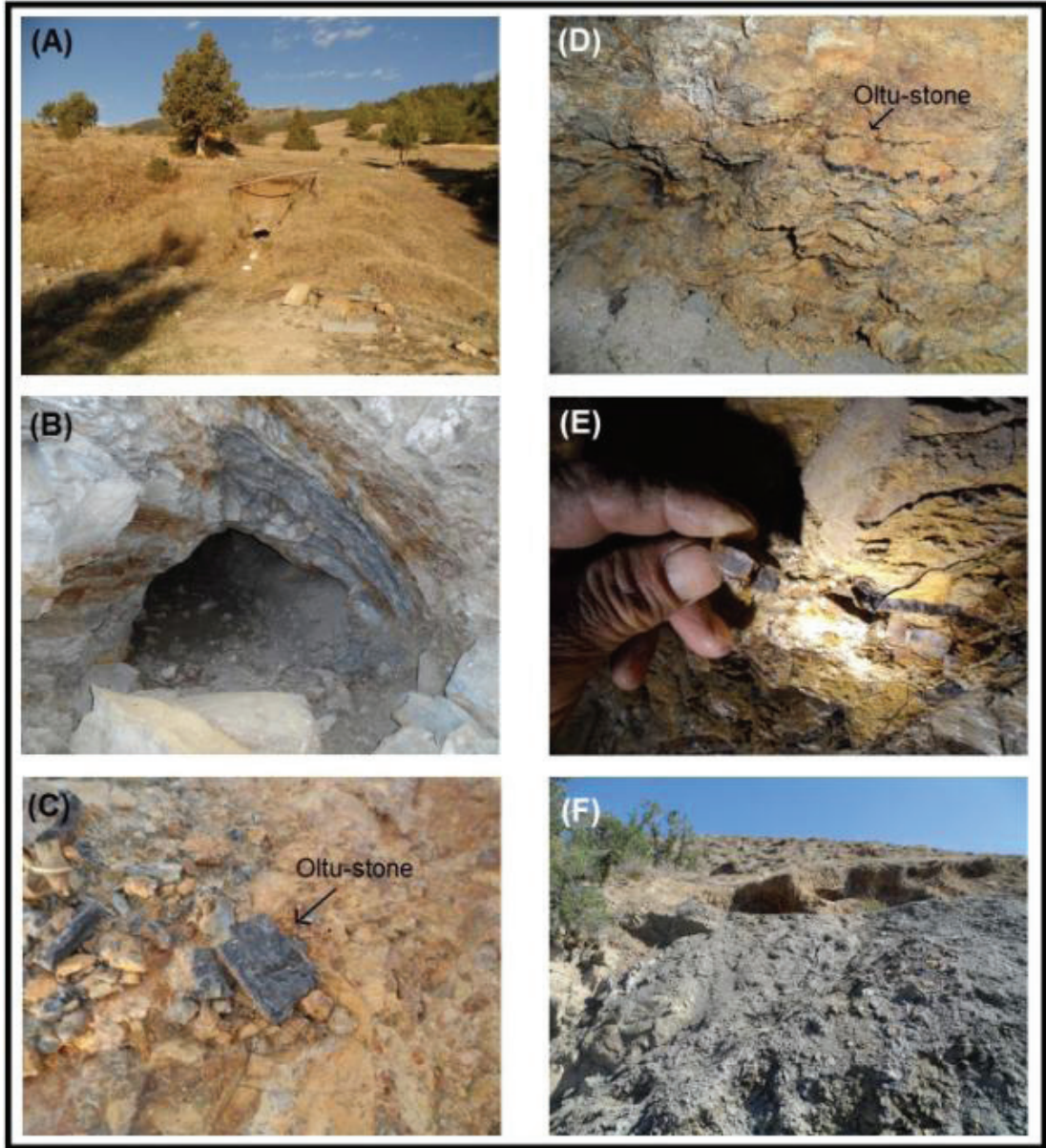


**Figure 2.** Oltu stone material is excavated in Tutlu, Güllüce, Güzelsu, and Gökçedere villages, especially. Out of the total 287 quarries in the central Tutlu region, about 120 quarries are still being worked (A), (B), and (C). The material is mined from mountainous areas perpendicular to the general surface with galleries 70-80 cm in diameter where only two or three miners can work. Oltu stone was deposited as stratiform layers between about 0.5 and 80 cm in thickness. However, these Oltu stone strata are no longer continuous, but are found in broken pieces about 20-30 cm in length (D) and (E). Discarded, low-quality Oltu stone is abandoned nearby (F).

**Şekil 2.** Oltu taşı malzemesi özellikle Tutlu, Güllüce, Güzelsu ve Gökçedere köylerinde çıkarılmaktadır. Tutlu merkez bölgesindeki toplam 287 ocaktan yaklaşık 120'sinde halen çalışılmaktadır (A), (B) ve (C). Malzeme, sadece iki veya üç madencinin çalışabildiği 70-80 cm çapındaki galerilerle genel yüzeye dik dağlık alanlardan çıkarılmaktadır. Oltu taşı, kalınlığı yaklaşık 0,5 ila 80 cm arasında değişen stratiform tabakalar halinde çöker. Bununla birlikte, bu Oltu taşı tabakaları artık sürekli değildir, ancak yaklaşık 20-30 cm uzunluğunda kırık parçalar halinde bulunur (D) ve (E). Atılmış, düşük kaliteli Oltu taşı yakınlarda terk edilmiştir (F).



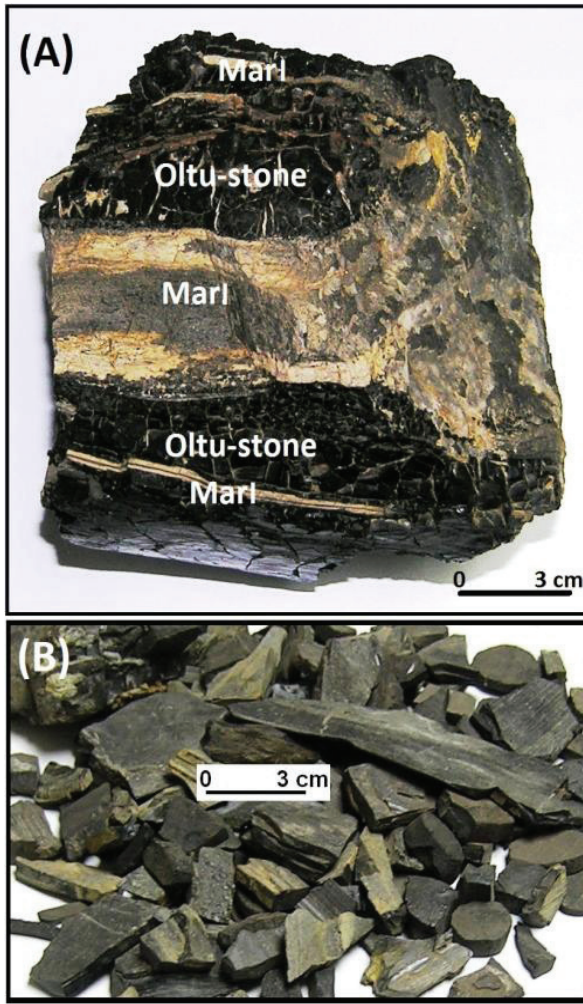


**Figure 3.** A block, including alternating Oltu stone material and the host rock, marl (A). The loose rough (unpolished) Oltu stones (B).

**Şekil 3.** Ardalanan Oltu taşı malzemesi ve ana kaya olan marndan yapıli bir blok (A). Gevşek kaba (cilalanmamış) Oltu taşları (B).

The region lies within a Jurassic-Cretaceous complex zone (the Olur-Tortum zone) that was fractured by tectonic events, and then separated into three geological units; the Olur, Aksu, and Çardaklı Units from northwest to southeast, respectively. The three units of the same age are all dissected along tectonic boundaries in the field. The slice containing Oltu stone belongs to the Olur Unit. Figure 4A represents the Olur

Slice of the Olur Unit only. Thus, only one of the three sliced units - the Olur Unit- includes the turbostratic carbonaceous Oltu stone. These three units (or tectonic slices) were then pushed into the Oltu-Balkaya Tertiary Basin to form the Oltu thrust zone. All these units were then cut by a dacitic intrusion in the Lower Eocene (Konak and Hakyemez, 2008). Thus, the sedimentary Oltu stones occur in the Upper Jurassic-Lower Cretaceous Olurdere Formation of the Olur Unit of the Olur-Tortum Zone (Figure 4A).

The base of the Olur Unit begins with intercalated alkaline, intermediate, and acidic volcanics of the Lower Jurassic. These volcanics are overlain by Middle Jurassic deltaic and marine fan clastics with a sharp contact. The clastics are followed by Upper Jurassic hemi-pelagic cherty carbonates, alternations of sandstone, siltstone and marl in the Lower Cretaceous and intermediate volcanics that laterally grade into the sandstones.

A shallow marine Liassic-Lower Malm sequence with volcano-sedimentary character overlies this basement above an angular unconformity. This unit is conformably overlain by Upper Jurassic-Lower Cretaceous limestones. The Hotnbian-Campanian flysch formed by rapid deepening of the environment during the middle Lower Cretaceous and was conformably deposited on the Upper Jurassic-Lower Cretaceous carbonates. The Upper Campanian and Lower Maastrichtian deposits are represented by volcanic and pelagic carbonates, respectively.

The upper part of the sequence contains marl and clayey limestone alternations of the Middle and Upper Cretaceous, followed by Lower Palaeocene neritic limestone and Upper Palaeocene marl and siltstone alternations with turbiditic sandstone and limestone interbeds. These were covered by terrestrial and shallow marine clastics in the Upper Eocene with an angular unconformity where horizontal layers cover sharply dipping beds. (Konak and Hakyemez, 2008) (Figure 4B).

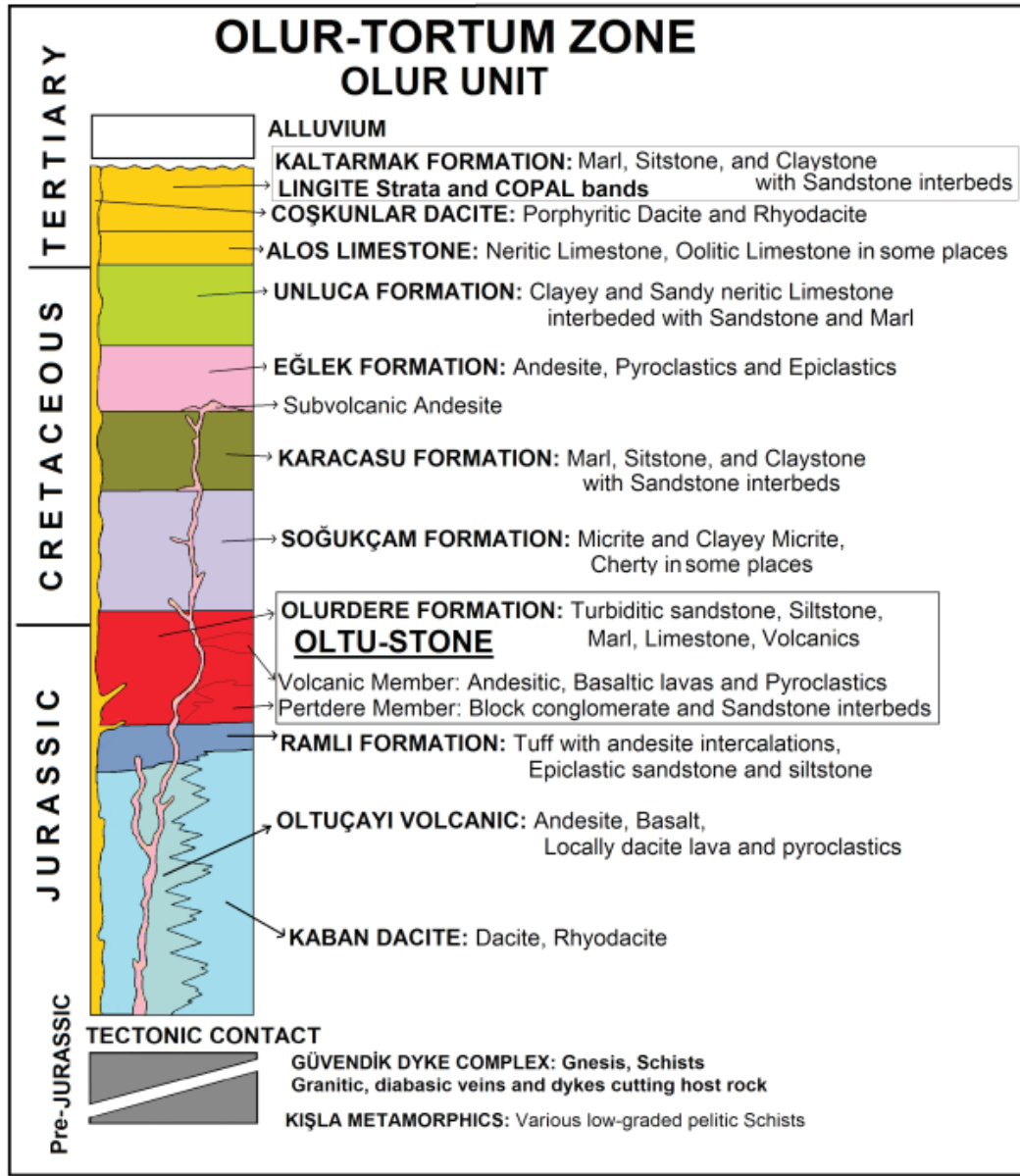


**Figure 4.A.** Simplified columnar section, representing the Olur unit including Oltu stone in the Olur-Tortum geological sequence from Oltu (Erzurum) (modified from Konak and Hakyemez, 2008).

**Şekil 4.A.** Oltu (Erzurum) civarındaki Olur-Tortum jeolojik istifinde Oltu taşı formasyonunu içeren Olur birimini temsil eden basitleştirilmiş kolon kesit (Konak ve Hakyemez, 2008'den değiştirilmiştir).

Oltu stones have been mined from the slopes of the Kırdag Mountains for about a century (Figures 1, 2 and 3). Many sites are located near the villages of Tutlu, Günlüce, Güzelsu, and Gökçedere in the Oltu-Erzurum region of Turkey.

There are approximately 600 quarries, of which at least 120 are still in operation (Figure 2). The identification of new sites for the extraction of Oltu stone is based on field observations and previous experiences.



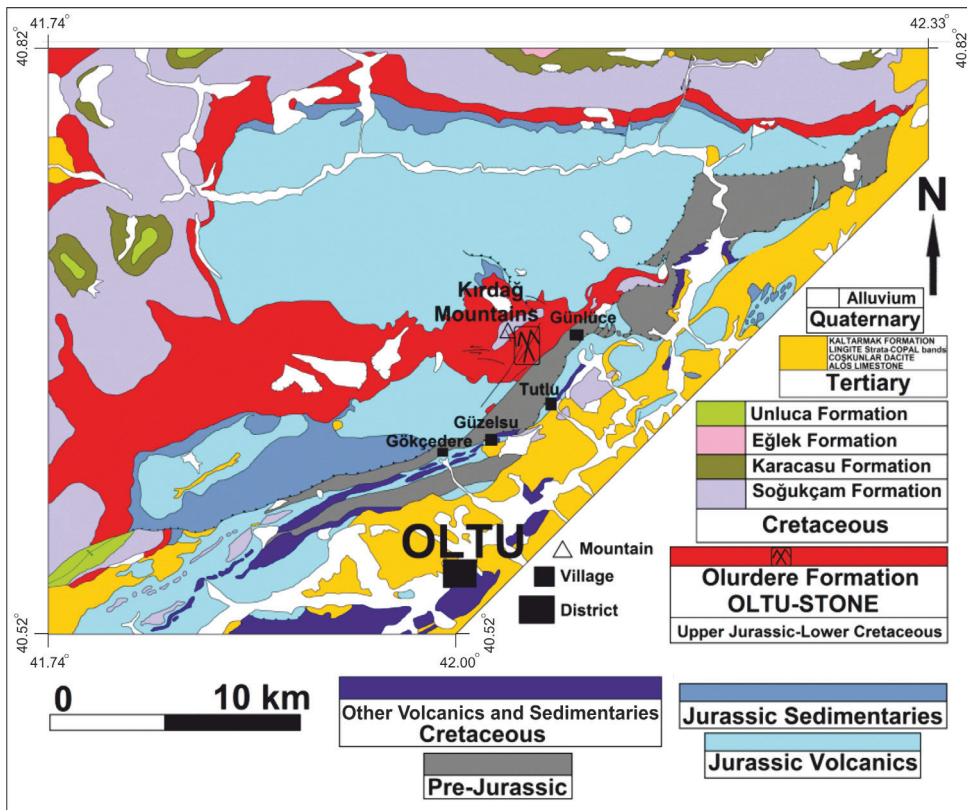


**Figure 4.B.** Simplified geological map of the Oltu-Erzurum region, including Gökçedere, Güzelsu, Tutlu, and Günlüce villages (modified from Konak and Hakyemez, 2008).

**Şekil 4.B.** Gökçedere, Güzelsu, Tutlu ve Günlüce köylerini kapsayan Oltu-Erzurum bölgesinin basitleştirilmiş jeoloji haritası (Konak ve Hakyemez, 2008'den değiştirilmiştir).

The material is mined in mountainous areas from vertical working surfaces with exposures of only 70-80 cm across that accommodate only two or three miners at a time. Most extraction is done by hand with short-handled shovels, hammers, and chisels. As the working face slopes inwards, waste is removed by four-wheeled wooden carts pulled by ropes (Bilgin et al., 2011).

When the depth of the working face reaches about 150 m or when unexpected situations occur that make working in the gallery unsafe, it is abandoned (Zengin, 1956; Çiftçi et al., 2002; Karayığit et al., 2002; Çiftçi et al., 2004; Karayığit, 2007; Bilgin et al., 2011; Kalkan et al., 2012) (Figure 2). This material was originally deposited

as horizontal strata alternating with marls between about 0.5 and 50 cm in thickness. However, the Oltu stone horizons (bands) are often no longer conformable to the original stratification but are broken up into sections about 20-30 cm in length (Figure 3A). According to geological field observations, the total reserve in the study area is estimated to be approximately 150,000 tonnes.

This material is unique and has some unusual mineralogical characteristics. The rough Oltu stone is generally of a dull to bright black colour, but sometimes it is blackish brown, grey, or greenish (Figure 3B). Oltu stone stays shiny as long as it is handled and does not react with human perspiration or leave marks on the skin.

## RESULTS

### Chemistry

The results of the chemical analysis of the representative Oltu stone are given in Table 1. Two important elements are noteworthy - carbon over 50% and sulphur only about 0.32%. If the

LOI value of 97.8% is considered, the initial carbon amount is very high in Oltu stone. This value is similar to those for synthetic carbon black varieties published before, such as, 97.7% for “unspecified carbon black”; 96.5% for “vulcan XC 72R”, 98.4% for “cabot fluffy”, and 95.5% for “regal 600” (Clague et al., 1999).

**Table 1.** Bulk and trace element chemical analyses of representative Oltu stones.

*Çizelge 1. Temsili Oltu taşlarının toplam ve eser element kimyasal analizleri.*

Bulk	Method	Detection limits	Oltu stone	Trace	Method	Detection limits	Oltu stone
SiO <sub>2</sub>	ME-ICP06	0.01%	1.57	Ag	ME-MS81	1 ppm	<1
Al <sub>2</sub> O <sub>3</sub>	ME-ICP06	0.01%	0.2	Ba	ME-MS81	0.5 ppm	8.8
Fe <sub>2</sub> O <sub>3</sub>	ME-ICP06	0.01%	0.5	Ce	ME-MS81	0.5 ppm	2.5
CaO	ME-ICP06	0.01%	0.28	Co	ME-MS81	0.5 ppm	3.6
MgO	ME-ICP06	0.01%	0.06	Cr	ME-MS81	10 ppm	20
Na <sub>2</sub> O	ME-ICP06	0.01%	0.05	Cs	ME-MS81	0.01 ppm	0.13
K <sub>2</sub> O	ME-ICP06	0.01%	0.04	Cu	ME-MS81	5 ppm	<5
Cr <sub>2</sub> O <sub>3</sub>	ME-ICP06	0.01%	<0.01	Dy	ME-MS81	0.05 ppm	0.91
TiO <sub>2</sub>	ME-ICP06	0.01%	0.03	Er	ME-MS81	0.03 ppm	0.46
MnO	ME-ICP06	0.01%	0.01	Eu	ME-MS81	0.03 ppm	0.16
P <sub>2</sub> O <sub>5</sub>	ME-ICP06	0.00%	0.08	Ga	ME-MS81	0.1 ppm	1.1
SrO	ME-ICP06	0.01%	<0.01	Gd	ME-MS81	0.05 ppm	0.83
BaO	ME-ICP06	0.01%	<0.01	Hf	ME-MS81	0.2 ppm	0.7
				Ho	ME-MS81	0.01 ppm	0.19
LOI	OA-GRA05	0.01%	97.8	La	ME-MS81	0.5 ppm	1
Total	TOT-ICP06	0.01%	100.5	Lu	ME-MS81	0.01 ppm	0.06
				Mo	ME-MS81	2 ppm	<2
C	C-IR07	0.01%	>50	Nb	ME-MS81	0.2	3.2
S	S-IR08	0.01%	0.32	Nd	ME-MS81	0.1 ppm	1.4
				Ni	ME-MS81	5 ppm	6
				Pb	ME-MS81	5 ppm	<5
				Pr	ME-MS81	0.03 ppm	0.32
				Rb	ME-MS81	0.2 ppm	2.5
				Sm	ME-MS81	0.03 ppm	0.46
				Sn	ME-MS81	1 ppm	<1
				Sr	ME-MS81	0.1 ppm	10.5
				Ta	ME-MS81	0.1 ppm	<0.1
				Tb	ME-MS81	0.01 ppm	0.14
				Th	ME-MS81	0.05 ppm	0.38
				Tl	ME-MS81	0.5 ppm	<0.5
				Tm	ME-MS81	0.01 ppm	0.08
				U	ME-MS81	0.05 ppm	0.23
				V	ME-MS81	5 ppm	175
				W	ME-MS81	1 ppm	4
				Y	ME-MS81	0.5 ppm	6
				Yb	ME-MS81	0.03 ppm	0.4
				Zn	ME-MS81	5 ppm	8
				Zr	ME-MS81	2 ppm	67

Other interesting aspects of the analyses include the relatively high concentration of silica (SiO<sub>2</sub>: 1.75 wt.%). In addition, higher than expected Ba (8.8 ppm) and V (175 ppm) concentrations, which are unusual for a coal material. The abundance of other trace elements, such as Sr (10.5 ppm), Th (0.38 ppm), U (0.23 ppm), and Zr (67 ppm), are also unexpectedly high. The abundance of trace elements is attributed to marine sedimentation and diagenesis. The composition strongly suggests that carbonaceous Oltu stone material is not an organic jet material transformed from wood, but rather an inorganic carbon material. Clague and colleagues (1999) found similar values for synthetic carbon blacks used in experiments on diesel engine soot (Clague et al., 1999). In addition, Yu and colleagues (1993) reported that the value of carbon in turbostratic carbon materials is very high (Yu et al., 1993).

### Specific Gravity

The hydrostatic balance (HB) method was used to analyse the specific gravity of the Oltu stone samples. The values, based on the formula ( $SG = \frac{W_{air}}{W_{air} - W_{water}}$ ), were measured as 1.317. In fact, this specific gravity value is higher from those of many coals and related blackish carbonaceous materials derived from fossil hydrocarbons. The typical specific gravity of Oltu stone is distinctive. Thus, measurement of specific gravity by the simple hydrostatic balance method is a powerful tool to distinguish this carbon black material from the other natural and synthetic carbon black materials and related blackish carbonaceous materials.

### X-Ray Diffraction (XRD)

Matching of numerical data obtained from XRD analyses of the Oltu stone samples with data for ideal carbonaceous materials (diamond, graphite, nanotubes etc.) compiled from the well-known database (RRUFF, 2013) and some related publications (Brown and Altermatt, 1985)

using a comparative matching technique was unsuccessful.

In the XRD pattern of Oltu stone (Figure 5), a total of 12 X-ray diffraction bands were acquired. The two higher bands centred at 4.20 and 3.78 Å, and the four relatively lower bands centred at 2.51, 2.28, 2.25, and 2.12 Å are characteristic. Two bands that developed between 21.5°-24° are ascribed to turbostratic carbon (Herrera-Alonso et al., 2007). In addition, six small bands centred at 14.79, 3.22, 3.05, 2.72, 1.95 and 1.69 Å also form part of the pattern.

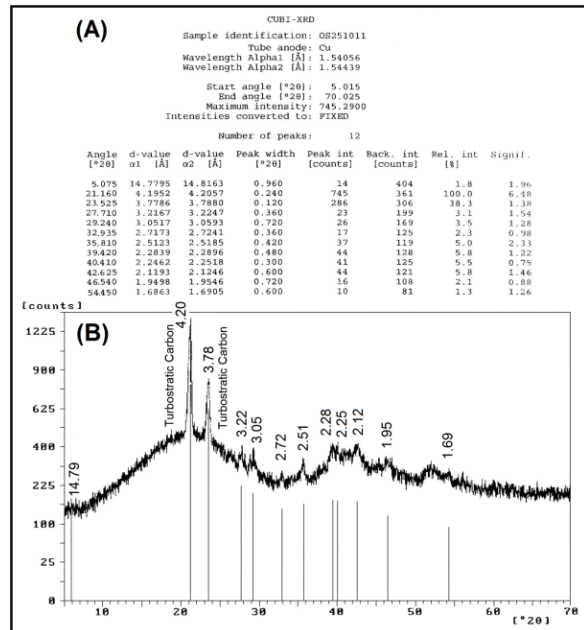


**Figure 5.** Tabular XRD data (a), the XRD pattern for representative Oltu stone (b). Two higher peaks centred at 4.20 and 3.78 Å and four smaller peaks centred at 2.51, 2.28, 2.25, and 2.12 Å are characteristic. Two peaks that developed between 21.5°-24° are ascribed to turbostratic carbon.

**Şekil 5.** Tabular XRD verileri (a), Oltu taşının temsili bir XRD deseni (b). Merkezi 4,20 ve 3,78 Å olan iki yüksek pik ve merkezleri 2,51, 2,28, 2,25 ve 2,12 Å olan dört küçük pik karakteristiktir. 21,5°-24° arasında gelişen iki pik turbostratik karbona atfedilir.

By eliminating the peaks due to inclusions (peaks at 2.51, 2.28, 2.25, and 2.12 Å are due to



silica; and peaks at 2.72 and 1.69 Å are due to pyrite), the peaks at 14.79, 4.20, 3.78, 3.22, 3.05, and 1.95 Å can be assigned to the carbonaceous material.

We believe that many of the XRD bands for Oltu stones reflect the packing distance of saturated structures. In addition, Oltu stones also contain some graphite-like structures (crystalline carbon). These observations suggest that the crystallites in the Oltu stone samples have intermediate structures between graphite and an amorphous state termed a turbostratic structure or random layer lattice structure (Tuinstra and Koenig, 1970; Hatipoğlu et al., 2012).

Ungar et al. (2002) investigated the microstructure of synthetic carbon blacks (N990, N774, and N134) by X-ray diffraction peak profile

analysis and concluded that there appears to be no difference between soot and carbon black from the point of view of morphology and internal structure (Lahaye and Prado, 1981; Clague et al., 1999). Hauptman et al. (2012) reported that X-ray photoelectron spectroscopy gives the oxygen content and the nature of functional groups on particle surfaces (Hauptman et al., 2012). In addition, in a previous study (Li et al., 2007), X-ray diffraction patterns of hexagonal graphite (h-graphite) and turbostratic carbon (t-carbon) were simulated by using the general Debye equation. The simulation results indicated that the diffraction angles and FWHMs of diffraction lines could not be simply used to characterise the lattice parameters and crystallite sizes of t-carbon (Li et al., 2007).

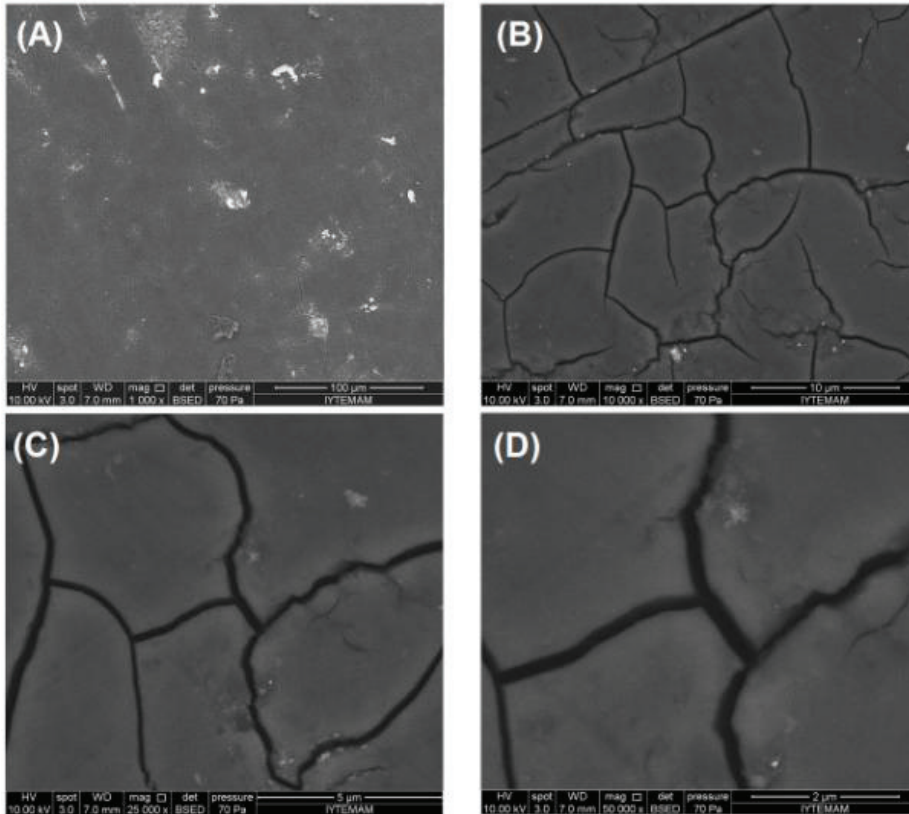


**Figure 6.** Four scanning electron microscope images (SEM) at 1,000x (A), 10,000x (B), 25,000x (C), and 50,000x (D) magnifications of Oltu stone obtained with backscattered electron detection.

**Şekil 6.** Oltu taşının geri saçılan elektron algılama ile elde edilen 1.000x (A), 10.000x (B), 25.000x (C) ve 50.000x (D) büyütmelelerdeki dört taramalı elektron mikroskobu görüntüsü (SEM).

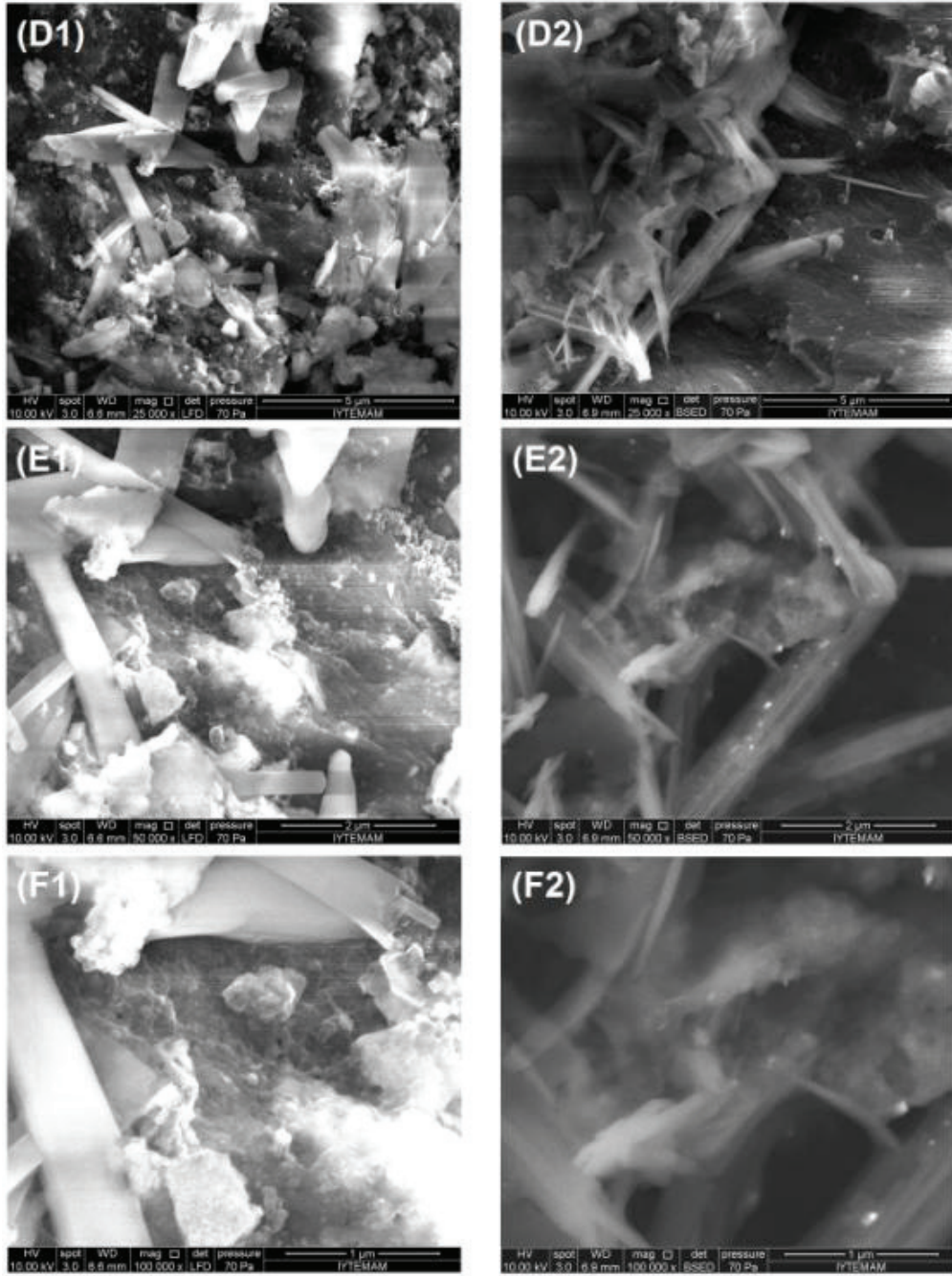


**Figure 7.** Six scanning electron microscope images (SEM) at magnifications of 25,000x (D1) and (D2), 50,000x (E1) and (E2), and 100,000x (F1) and (F2) of Oltu stone. The left column was imaged with a large field detector; the right column with a backscattered electron detector. Scanning electron micrographs of carbonaceous Oltu stone clusters show the typical elongated habit.

**Şekil 7.** Oltu taşının 25.000x (D1) ve (D2), 50.000x (E1) ve (E2) ve 100.000x (F1) ve (F2) büyütmelerde altı taramalı elektron mikroskobu görüntüsü (SEM). Sol sütun geniş alan dedektörü ile görüntülenmiştir; sağ sütun geri saçılan elektron dedektörü ile görüntülenmiştir. Karbonlu Oltu taşı kümelerinin taramalı elektron mikrografları tipik uzun yapısını göstermektedir.

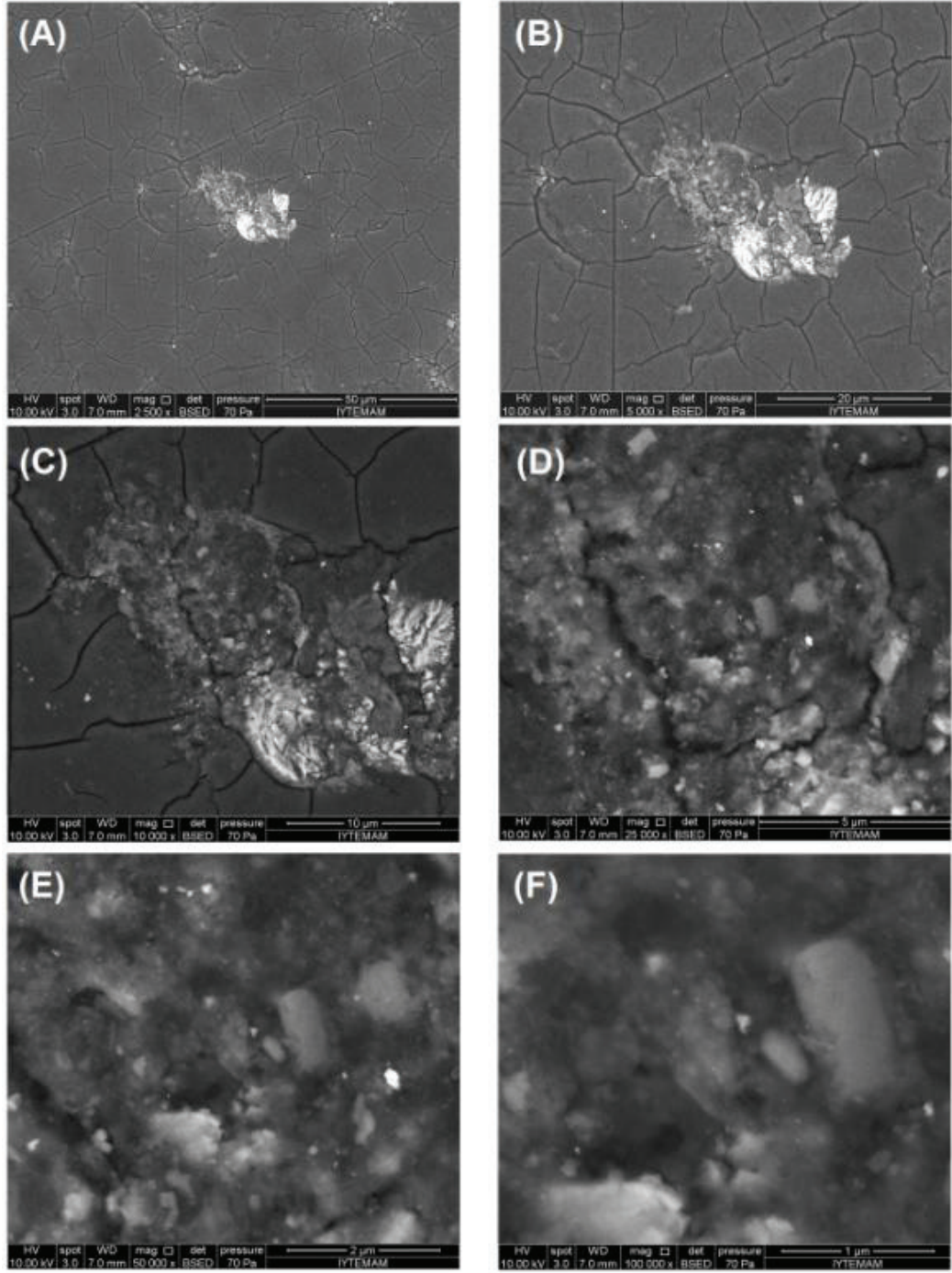


**Figure 8.** Six scanning electron microscope images (SEM) at magnifications of 2,500x (A), 5,000x (B), 10,000x (C), 25,000x (D), 50,000x (E), and 100,000x (F) for Oltu stone. The left column was imaged with a large field detector; the right column, with a backscattered electron detector.

**Şekil 8.** Oltu taşının 2.500x (A), 5.000x (B), 10.000x (C), 25.000x (D), 50.000x (E) ve 100.000x (F) büyütmelerde altı taramalı elektron mikroskobu görüntüsü (SEM). Sol sütun geniş alan dedektörü ile görüntülenmiştir; sağ sütun ise geri saçılan elektron dedektörü ile görüntülenmiştir.



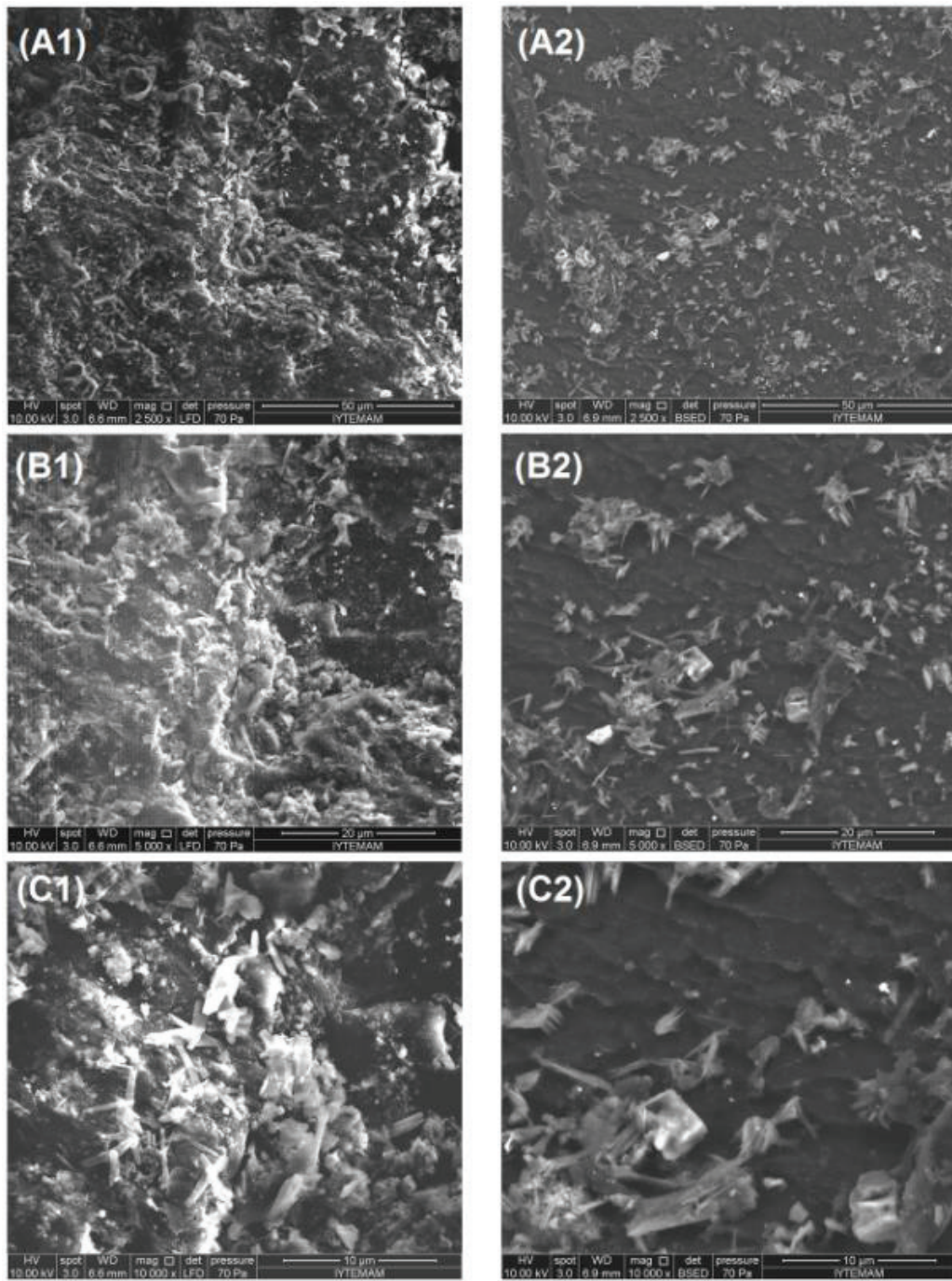


**Figure 9.** Six scanning electron microscope images (SEM) at magnifications of 2,500x (A1) and (A2), 5,000x (B1) and (B2), and 10,000x (C1) and (C2) for Oltu stone. The left column was imaged with a large field detector; the right column, with a backscattered electron detector.

**Şekil 9.** Oltu taşının 2.500x (A1) ve (A2), 5.000x (B1) ve (B2) ve 10.000x (C1) ve (C2) büyüttmelerde altı taramalı elektron mikroskobu görüntüsü (SEM). Sol sütun geniş alan dedektörü ile görüntülenmiştir; sağ sütun ise geri saçılan elektron dedektörü ile görüntülenmiştir.

## Scanning Electron Microscopy (SEM)

Many scanning electron microscope images (SEM) of Oltu stone were acquired, and they are collected into four groups (Figures 6, 7, 8, and 9), that all show that the carbonaceous Oltu stone clusters have typical elongated habit.

The SEM images show that the internal structures of the carbonaceous Oltu stone consist of mostly small micron-sized (1.0 – 1.2  $\mu\text{m}$ ) and partially large nano-sized (900 – 1000 nm) carbon particles.

## Atomic Force Microscopy (AFM)

The AFM micrographs were taken as two different three-dimensional (3-D) morphologies (Figure 10A and B) and one two-dimensional (2-D) graphic (Figure 10C) for Oltu stone. In the 3-D surface topographies, black zones show dips, and white points show high zones.

A 62.3 $\times$ 62.3- $\mu\text{m}$  face of Oltu stone was scanned. The topography map shows maximum and minimum level of indentation and projection. The grain sizes of the carbonaceous matrix range from a minimum of 900 nm to a maximum of 1.2  $\mu\text{m}$ .

## Oxygen Isotopes

The  $\delta^{18}\text{O}$  values were between +37.2‰ and +40.8‰ (SMOW) for Oltu stone, and between +10.3‰ and +12.3‰ (SMOW) for the enclosing flysch. The values demonstrate that the strata of Oltu stone formed during diagenesis at a low temperature of around 50 °C. On the other hand, the surrounding flysch rocks formed at higher temperature, perhaps above 100 °C. We can compare the results to estimate the sedimentation period of the co-existent Oltu stone material and flysch rock.

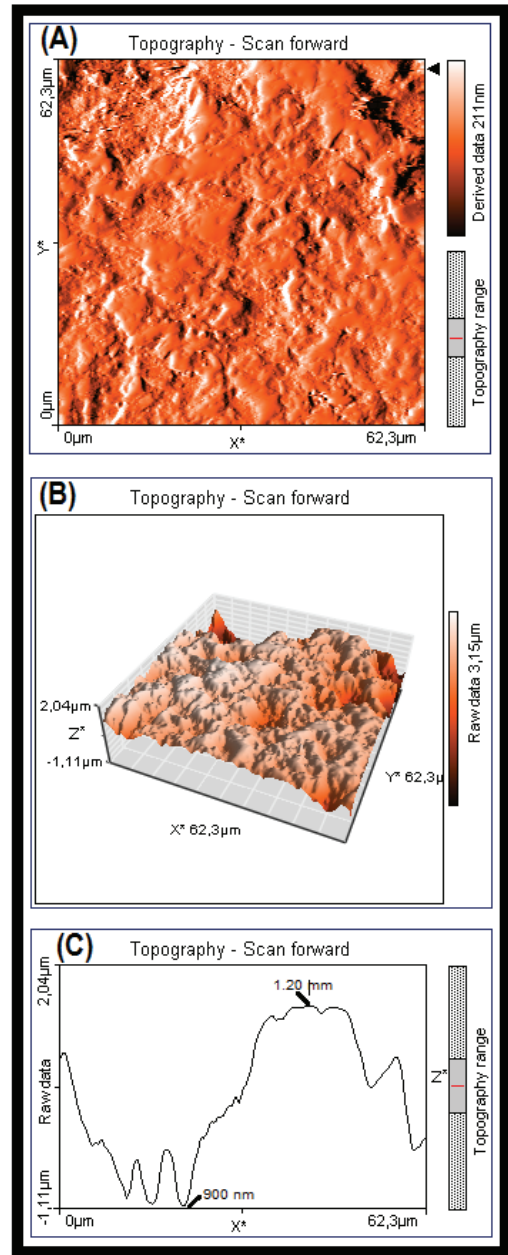


**Figure 10.** AFM micrographs taken from two different 3-D morphologies (A) and (B), and one 2-D graphic (C) for Oltu stone. The grain sizes of the matrix components have a minimum size of 900 nm and a maximum size of 1.2  $\mu\text{m}$ .

**Şekil 10.** Atomik kuvvet mikroskobu (AFM) mikrografları Oltu taşı için iki farklı 3-D (üç boyutlu) morfolojiden (A) ve (B) ve bir 2-D (iki boyutlu) grafikten (C) alınmıştır. Matris bileşenlerinin tane boyutları minimum 900 nm ve maksimum 1,2  $\mu\text{m}$ 'dir.

Kolodny and Epstein (1976) stated that deep sea cherts of all ages show a spread of  $\delta^{18}O$  values, with increasing diagenesis being reflected in a lowering of  $\delta^{18}O$ . The  $\delta^{18}O$  of deep-sea cherts generally decrease with increasing age, indicating an overall cooling of the ocean bottom during the last 150 my in geological time. The  $\delta^{18}O$  of chert ranges between 27 and 39 per mil relative to SMOW,  $\delta^{18}O$  of porcellanite—between 30 and 42 per mil. Accordingly, the consistent enrichment of opal-CT in porcellanite in  $^{18}O$  with respect to coexisting microcrystalline quartz in chert is probably a reflection of a different temperature (depth) of diagenesis of the two phases.

When the chemical contents of Oltu stone regarding  $SiO_2$  of 1.57% are considered (Table 1), we can conclude that the value of average +39 of SMOW for Oltu stone can explain its relatively

higher silica content. In addition, the value of +13.3 of SMOW for the surrounding flysch may be evidence to indicate its depositional period was Upper Jurassic-Lower Cretaceous.

### Thermogravimetry (DTA/TGA)

Thermogravimetric behaviours including thermal properties and thermal stability of Oltu stone, and some associated mineral inclusions, were studied by thermogravimetric analyses (TGA). The transformations and/or decomposition of the carboniferous building blocks and/or paramorphism of other inclusion minerals during the heating process can be also determined by differential thermal analyses (DTA). Accordingly, simultaneous DTA/TGA glow curves are given in Figure 11.

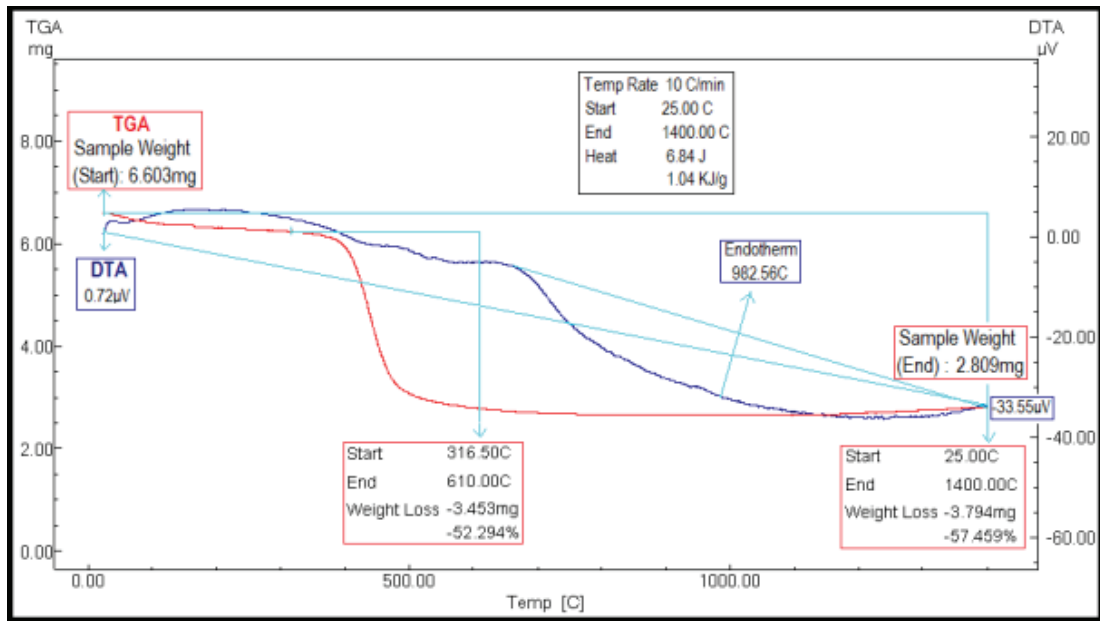


**Figure 11.** DTA/TGA pattern for Oltu stone. Measurements were simultaneous. The TGA glow curve was corrected for buoyancy of the atmosphere. The drift observed in the dotted red lines is typical of the effect of buoyancy. Mass loss measurements were corrected in the red line, because apparent mass gain is an experimental artefact.

**Şekil 11.** Oltu taşının diferansiyel termal analiz ve termogravimetrik analiz (DTA/TGA) modeli. Ölçümler eş zamanlı olarak yapılmıştır. TGA kızdırma eğrisi atmosferin kaldırma kuvveti için düzeltilmiştir. Noktalı kırmızı çizgilerde gözlemlenen kayma, kaldırma kuvvetinin etkisinin tipik bir örneğidir. Kütle kaybı ölçümleri kırmızı çizgide düzeltilmiştir çünkü görünür kütle kazancı deneysel bir artiftaktır.



During heating to 1400 °C, the glow curves indicate that the weight loss of Oltu stone is due to carboniferous material loss only, and this loss occurs in the temperature ranges between about 316.5 and 610.0 °C. In addition, after making some corrections for the artefactual mass gain observed due to drift from the buoyancy effect of the atmosphere in the TGA glow curve, Oltu stone had a total mass loss of 57.46% (TGA glow curve), and one distinctive sharp endotherm at 982.56 °C and three weaker endotherms (DTA glow curve). The main thermogravimetric weight loss was about 52% at 316.5 °C, and the last weight loss is about 2% at 1400 °C. This result shows that Oltu stone has a relatively higher resistance to overheating.

The pattern of the simultaneous differential thermal and thermal gravimetric analyses of Oltu stone displays slight differences compared to synthetic carbon blacks.

The TGA tests show that care should be taken not to exceed temperature above 316 °C if the material is used for industrial purposes. This value can also be accepted as the starting point of decomposition. The decomposition starting point for Oltu stone seems to be slightly lower than those of synthetic carbon blacks; however, there seems to be no data in the literature for similar natural materials found in other localities around the world for comparison. The TGA result can be attributed to the presence of higher crystallinity in Oltu stone.

The TGA tests show that the total mass loss percentage for Oltu stone was found to be less than about 57%, in contrast to other synthetic carbon blacks (up to 65%). This may be related to silica inclusions (Table 1). The DTA tests show that Oltu stone was fully decomposed or transformed at about 679 °C, probably through formation of high temperature paramorphs. Thus, we also conclude that decomposition at moderate temperatures is entirely due to phase transformations.

Ungar et al. (2002) stated that heat treatment results in increased vertical and lateral sizes of graphitic crystallites. The dislocation density increases during annealing. Concentration of amorphous carbon is decreased after heat treatment. They interpreted this observation because of amorphous carbon being gradually incorporated into graphitic layers.

### Micro-Raman Spectroscopy

For confocal (532 nm green laser) micro-Raman spectra, a typical micro-Raman spectrum of the material is given in Figure 12. Raman spectra for Oltu stone were recorded between 50 and 3200  $\text{cm}^{-1}$ : measurements over a wide spectral range showed, important peaks at 1346  $\text{cm}^{-1}$  and 1585  $\text{cm}^{-1}$  in the spectral range between 1000 and 1800  $\text{cm}^{-1}$  characteristic of the para-crystallites, other features ascribed to amorphous regions in the range between 2500 and 3000  $\text{cm}^{-1}$ , and finally, the main inclusions revealed by XRD and chemical analyses, quartz and pyrite, produce the enhanced background between 200 and 500  $\text{cm}^{-1}$  in these spectra probably related to  $\text{SiO}_2$ , and the higher peak at about 100  $\text{cm}^{-1}$  probably related to  $\text{FeS}_2$ .

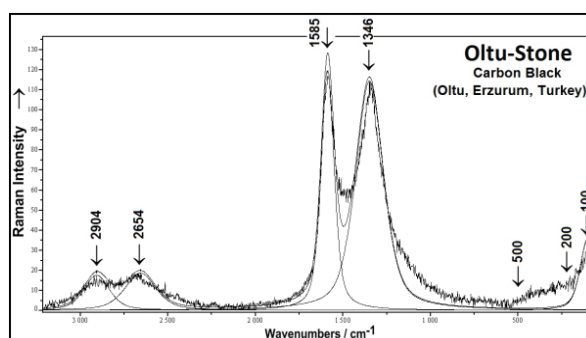


**Figure 12.** Raman vibrational bands for representative Oltu stone. Two important peaks at 1346  $\text{cm}^{-1}$  and 1585  $\text{cm}^{-1}$  in the spectral range between 1000 and 1800  $\text{cm}^{-1}$  are characteristic of quasi-crystallites, other features are ascribed to amorphous regions in the range between 2500 and 3000  $\text{cm}^{-1}$ , and finally, the enhanced background between 200 and 500  $\text{cm}^{-1}$  in these spectra

could be related to ( $\text{SiO}_2$ ), and the higher peak at about  $100\text{ cm}^{-1}$  could be related to ( $\text{FeS}_2$ ) as the main inclusions (adapted from Hatipoğlu et al. 2012).

**Şekil 12.** Raman titreşim bantları Oltu taşını temsil etmektedir. Spektral aralıkta  $1000$  ile  $1800\text{ cm}^{-1}$  arasında  $1346\text{ cm}^{-1}$  ve  $1585\text{ cm}^{-1}$ 'deki iki önemli pik, yarı-kristalitlerin karakteristiğidir;  $2500$  ile  $3000\text{ cm}^{-1}$  arasındaki amorf bölgelere atfedilen diğer özellikler ve son olarak, ana kapanımlar, bu spektrumlarda  $200$  ile  $500\text{ cm}^{-1}$  arasındaki artmış arka plan ( $\text{SiO}_2$ ) ile ilişkili olabilir ve yaklaşık  $100\text{ cm}^{-1}$ 'deki daha yüksek pik ( $\text{FeS}_2$ ) ile ilişkili olabilir (Hatipoğlu ve ark. 2012'den uyarlanmıştır).

The two main G bands at  $1346\text{ cm}^{-1}$  ( $A_{1g}$ ) and  $1585\text{ cm}^{-1}$  ( $E_{2g}$ ) are characteristic of micro-crystallites (graphite) whereas the Raman peaks at  $2654$  and  $2904\text{ cm}^{-1}$  were ascribed to the amorphous carbon regions on the surface. The last peaks have the “signature” of a  $\text{sp}^n$  bonded carbon. This  $\text{sp}^n$  nomenclature represents carbon in highly dislocated graphitic type species (Brown and Altermatt, 1985). The  $\text{sp}^3$  bonds are found to coexist with  $\text{sp}^2$  bonds in the turbostratic carbon materials. The  $\text{sp}^3$  bonds in turbostratic carbon provide nucleation sites for diamond crystals and improve the nucleation rate at the early stage of deposition of diamond on turbostratic carbon (Yu et al, 1993). Therefore, Oltu stones are very suitable materials on which to deposit diamond film coatings. Finally, the enhanced background between  $250$  and  $400\text{ cm}^{-1}$  could be associated with the presence of pyrite. We conclude that micro-Raman spectroscopy investigations indicate that Oltu stone (natural carbon black) crystallites are non-spherical flat discs. A similar result was reported by Ungar et al (2005). In the synthetic carbon black powder samples, there was strong overlap of the diffraction profiles. The overlapping peaks had to be separated since the present evaluation method was worked out for individual profiles (Ungar et al., 2005).

Gruber et al. (1994) acquired Raman spectra for regular and heat-treated carbon blacks

determining the changes in microstructure due to thermal treatment at five heat-treatment temperatures ranging from room temperature to  $3000\text{ K}$ . They reported that the peak at  $1345\text{ cm}^{-1}$ , which was assigned to symmetric C-C vibrations, was characteristic of disordered structures and its intensity decreased with increasing size of the graphitic planes. This band and the  $1575\text{ cm}^{-1}$  peak characteristic of graphite were analysed, and the ratio of their integrated intensities used to estimate the in-plane dimensions of graphitic crystalline regions and show that the size of these microcrystallites increases with temperature (Gruber et al., 1994).

In a high-pressure Raman and neutron scattering study of carbon black and highly oriented pyrolytic graphite, Zerda et al. (2000) reported that carbon black particles were composed of graphitic micro- or nano-crystallites and unknown amorphous carbon. A pressure induced frequency shift of the  $E_{2g}$  bands in various carbon blacks can be interpreted in terms of a modified intermolecular potential. Hauptman et al. (2012) suggested that Raman spectroscopy provides a measure of the relative amounts of disordered, graphitic and amorphous phases, and the lateral size of crystallites.

The synthetic carbon sample obtained from pyrolysis by GC-MASS (Lin, 2002) exhibits a Raman pattern like that of natural carbon black. Similar Raman results were reported in previous papers (Wang et al., 1994; Jawhari et al., 1995; Zerda et al., 2000) and in a mineral database (RRUFF, 2013), while original graphite exhibits a different spectrum (Tuinstra and Koenig, 1970). Ungar et al. (2002) stated that Raman measurements in synthetic carbon blacks indicate they have smaller crystallites than those measured by X-rays because the Raman spectra were mainly derived from the outer skin of the aggregates while X-ray diffraction detects crystallites throughout the volume of the sample.

When compared to the dispersive confocal micro-Raman spectra of all other kinds of carbon materials, the spectra of two different Oltu stone materials closely match the spectrum of carbon black (Figure 13).

### Industrial Usage of Turbostratic Carbon Materials

The most important usage of turbostratic carbon materials is as a surface for diamond film coatings. For example, Yu et al. (1993) showed how diamond films were grown on turbostratic carbon pre-grown on Cu substrates by hot filament chemical vapour deposition. The authors stated that to characterise both the turbostratic carbon and the diamond films, Auger electron spectroscopy, Raman spectroscopy, X-ray diffraction, infrared absorption spectroscopy, and scanning electron microscopy should be carried out. They concluded that the turbostratic carbon films could form on Cu at low temperatures ( $\approx 650^\circ\text{C}$ ) with the catalysis of Mo and that diamond crystallites formed rapidly on turbostratic carbon in less than 10 min at higher temperature ( $\approx 1000^\circ\text{C}$ ) (Yu et al, 1993).

### DISCUSSION and CONCLUSION

This study demonstrates that Oltu stone is an abiotic carbon black, and the source of the carbon is almost certainly Jurassic volcanism. Semi-graphitization of solid carbon of pyrogenous origin is a two-step process: first, the carbon of a sample of interest is oxidized to  $\text{CO}_2$ , and second, the  $\text{CO}_2$  is reduced to graphitic materials, like turbostratic carbon (Lahaye and Prado, 1981; Herrera-Alonso et al., 2007).

Oltu stone is a material composed essentially of elemental carbon in the form of quasi-spherical particles that are fused together into aggregates (Bansal and Donnet, 1993; Clague et al., 1999).

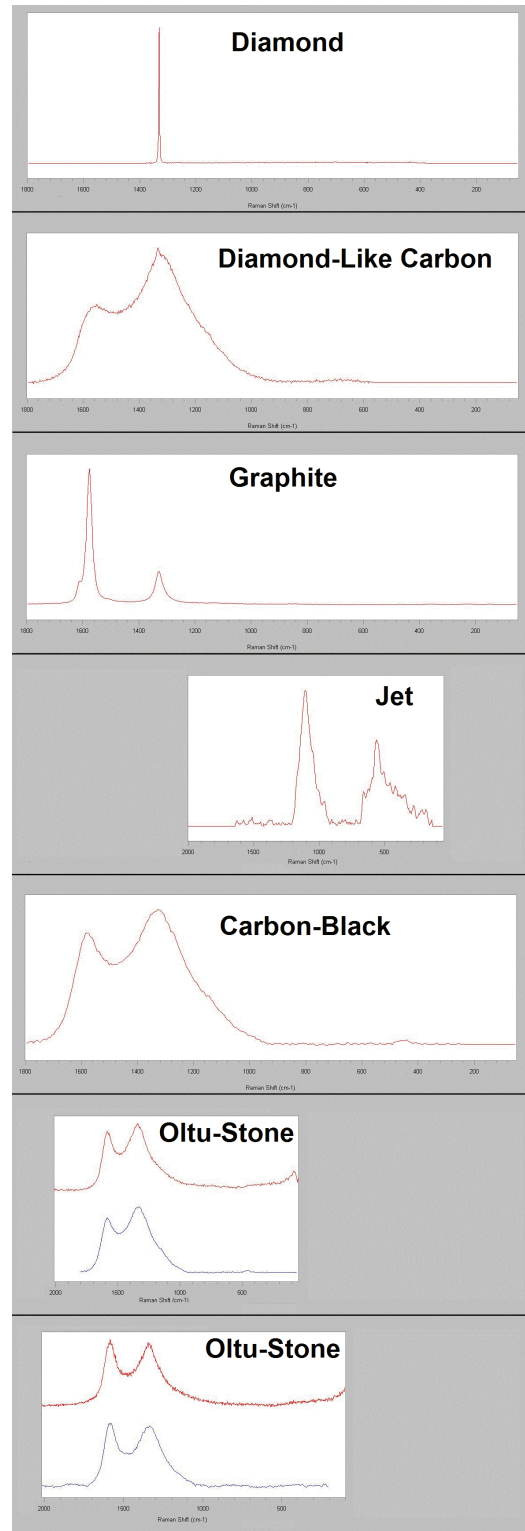


**Figure 13.** Dispersive confocal micro-Raman spectra for all kinds of carbon materials including Oltu stone

for comparison and contrast. All spectra were obtained from the same spectrometer.

**Şekil 13.** Karşılaştırma ve kontrast için Oltu taşı da dahil olmak üzere her türlü karbon malzemenin dağınık eşodaklı mikro-Raman spektrumları. Tüm spektrumlar aynı spektrometreden elde edilmiştir.

The geochemical formation of Oltu stone probably incorporated many of the features common to the thermal oxidative decomposition processes in a sedimentation basin. Partial combustion or thermal decomposition of hydrocarbons resulted in carbon dioxide, which was then redeposited higher in the geological column as inorganic layers of bituminous crystallites alternating with marl strata. Specifically, it is not the result of *in situ* processing of fossil resin (copal) or jet from fossilized wood, as mistakenly inferred by some previous authors (Zengin, 1956; Çiftçi et al., 2002; Karayığıt et al., 2002; Çiftçi et al., 2004; Karayığıt, 2007; Kalkan et al., 2012).

Many papers were published about Oltu stone, and none contains the detailed analytical data presented here. In addition, detailed geological field observations were undertaken to understand of its occurrence. Previously, it was claimed that ordinary coals and Oltu stones in the Oltu-Erzurum region are like carbonaceous materials, and that they were derived from fossil plants, largely on the basis that these materials are found next to each other in this region, even though they were deposited in the different geological periods. Oltu stone has a turbostratic structure intermediate between graphite and occurs in amorphous states. The formation of Oltu stone can be considered to incorporate many of the features common to thermal oxidative decomposition processes. We conclude that this material is composed essentially of elemental carbon in the form of tabular particles. Thus, the northern Oltu region contains two very different carbonaceous materials. One of them is the coal formation in Tertiary sedimentary units, which is directly derived from fossil organic hydrocarbons. The other is the Oltu stone formation in the Jurassic-Cretaceous flysch that

has abiotic origin, having formed from carbon dioxide.

Chemical and analytical investigations of Oltu stone reveal many essential fingerprints that indicate its origin and are useful for confirming its provenance. An LOI value of 97.8% shows that the initial carbon amount is the highest of any carbon black sample tested. In addition, SiO<sub>2</sub> of 1.57%, Fe<sub>2</sub>O<sub>3</sub> of 0.50%, and S of 0.32% are unusual impurities. The remarkable abundance of trace elements, including Sr (10.5 ppm), Th (0.38 ppm), U (0.23 ppm), and Zr (67 ppm), is consistent with an abiotic origin for Oltu stone and is not consistent with formation from processed fossil organic material.

We believe that Oltu stone is a mineral characterised by X-ray diffraction (XRD) as being a semi-crystalline (or pseudo-crystalline, or paracrystalline) material, so called turbostratic carbon. The two higher bands centred at 4.20 and 3.78 Å that develop between 21.5°-24° are ascribed to the turbostratic carbon. Additionally, the four smaller bands centred at 2.51, 2.28, 2.25 and 2.12 Å are specific to Oltu stone, but are not ascribed to any element.

In the SEM images, the internal structures are thinner, and they consist of sub-micron-sized (1.0 – 1.2 µm) and upper nano-sized (900 nm – 1.0 µm) carbon-building particles and some inclusions.

Similar particle sizes are confirmed by 3-D and 2-D graphics from AFM. The grain sizes of the matrix components display a size range with a minimum of 900 nm and a maximum of 1.2 µm.

The oxygen isotopic value of average +39 per mil relative to SMOW for Oltu stone can explain its relatively high silica content (1.57 wt.%). In addition, the oxygen isotopic value of +13.3 per mil relative to SMOW for the surrounding flysch indicates it was deposited in the Upper Jurassic-Lower Cretaceous.

In the simultaneous DTA/TGA glow curves, the main thermogravimetric weight loss was about 52% at 316.5 °C, and the total weight loss was



about 57% at 1400 °C. These results show that the material components of Oltu stone have relatively higher resistance to overheating in industrial applications.

We conclude that the carbonaceous Oltu-stone materials are not a fossil resin (copal) or jet material derived from fossilized wood as mistakenly inferred by some authors. Turbostratic carbon materials are important for industrial usage in the world. The  $sp^3$  bonds in the Oltu-stone coexist with  $sp^2$  bonds. The  $sp^3$  bonds can provide nucleation sites for diamond crystals and can improve the nucleation rate during the early stage of deposition of diamond coatings.

## GENİŞLETİLMİŞ ÖZET

*Bu çalışma, Türkiye'nin en önemli turbostratik karbonlu malzemesi olan Oltu taşının jeolojik, mikroyapısal, oksijen izotopik ve termogravimetrik incelemelerine odaklanmaktadır.*

*Oltu-taşının abiyotik bir karbon siyahı olduğunu ve karbon kaynağının kesinlikle Jura volkanizması olduğunu göstermektedir. Pirojen kökenli katı karbonun yarı grafitleşmesi iki aşamalı bir süreçtir: ilk olarak, ilgilenilen bir numunenin karbonu  $CO_2$ 'ye oksitlenir ve ikinci olarak  $CO_2$  daha sonra turbostratik karbon gibi grafitik malzemelere indirgenir (Lahaye ve Prado, 1981; Herrera-Alonso vd., 2007).*

*Oltu-taşı, esasen, agregalar halinde birbirine kaynaşmış yarı-küresel parçacıklar şeklinde elementel karbondan oluşan bir malzemedir (Bansal ve Donnet, 1993; Clague vd., 1999). Oltu-taşının jeokimyasal oluşumu muhtemelen bir çökeltme havzasındaki termal oksidatif ayrışma süreçlerinde ortak olan özelliklerin çoğunu içermektedir. Hidrokarbonların kısmi yanması veya termal ayrışması karbondioksit ile sonuçlanmış ve bu karbondioksit daha sonra jeolojik sütunda marn tabakaları ile dönüşümlü olarak bitümlü kristalitlerin inorganik katmanları şeklinde yeniden oluşmuştur. Özellikle, önceki bazı yazarların (Zengin, 1956; Çiftçi vd., 2002;*

*Karayiğit vd., 2002); Çiftçi vd., 2004; Karayiğit, 2007; Kalkan vd., 2012) belirttiği gibi fosil reçinenin veya fosilleşmiş ağaçtan gelen kara kehribarın yerinde işlenmesinin sonucu değildir.*

*Oltu taşı hakkında birçok makale yayınlanmıştır ve bunlardan hiçbiri burada sunulan ayrıntılı analitik verileri içermemektedir. Ek olarak, bu taşın oluşumunu anlamak için detaylı jeolojik saha gözlemleri yapılmıştır. Daha önce, Oltu-Erzurum bölgesindeki doğal kömürlerin ve Oltu taşlarının karbonlu malzemelere benzediği ve farklı jeolojik dönemlerde çökelmiş olsalar da bu malzemelerin bu bölgede yan yana bulunmalarına dayanarak fosil bitkilerden türetildikleri iddia edilmiştir. Oltu taşı, grafit arasında turbostratik bir yapıya sahiptir ve amorf olarak ortaya çıkar. Oltu-taşının oluşumunun, termal oksidatif ayrışma süreçlerinde yaygın olan özelliklerin çoğunu içerdiği düşünülebilir. Bunun esasen tabular parçacıklar şeklinde elementel karbondan oluşan bir malzeme olduğu sonucuna varılmıştır. Dolayısıyla, kuzey Oltu bölgesi birbirinden çok farklı iki karbonlu malzeme içermektedir. Bunlardan biri, doğrudan fosil organik hidrokarbonlardan türetilen Tersiyer tortul birimlerindeki kömür oluşumudur. Diğeri ise karbondioksitten oluşan abiyotik kökenli Jura-Kretase flišindeki Oltu taşı oluşumudur.*

*Oltu taşının kimyasal ve analitik incelemeleri, kökenini gösteren ve kaynağını doğrulamak için yararlı olan birçok temel parmak verilerini ortaya koymaktadır. 97,8'lik bir LOI değeri, başlangıçtaki karbon miktarının test edilen karbon siyahı örnekleri arasında en yüksek olduğunu göstermektedir. Ayrıca, %1,57'lik  $SiO_2$ , %0,50'lik  $Fe_2O_3$  ve %0,32'lik S olağandışı safsızlıklardır. Sr (10,5 ppm), Th (0,38 ppm), U (0,23 ppm) ve Zr (67 ppm) gibi eser elementlerin dikkate değer bolluğu, Oltu taşı için abiyotik bir kökenle tutarlıdır ve işlenmiş fosil organik malzemeden oluşumu tutarlı değildir.*

*Oltu taşının, X-ışını kırınımı (XRD) ile yarı-kristalin (veya sözde-kristalin veya para-kristalin) bir malzeme olarak karakterize edilen*

ve turbostratik karbon olarak adlandırılan bir mineral olduğu öngörülmektedir. 21,5°-24° arasında gelişen 4,20 ve 3,78 Å merkezli iki yüksek pik turbostratik karbon elementine atfedilir. Ayrıca, 2.51, 2.28, 2.25 ve 2.12 Å merkezli dört küçük pik Oltu taşına özgüdür, ancak herhangi bir elemente atfedilmemiştir.

Taramalı elektron mikroskobu (SEM) görüntülerinde, iç yapıların daha ince olduğu ve mikron altı (1,0 - 1,2 µm) ve üst nano boyutlu (900 nm - 1,0 µm) karbon yapı parçacıklarından ve bazı inklüzyonlardan oluştuğu görülmektedir.

Benzer partikül boyutları atomik kuvvet mikroskobunun (AFM) 3-D ve 2-D grafikleriyle doğrulanmıştır; matris bileşenlerinin tane boyutları minimum 900 nm ve maksimum 1.2 µm'lik bir boyut aralığı göstermektedir.

Oltu taşı için SMOW'a göre mil başına ortalama +39 olan oksijen izotopik değeri, nispeten yüksek silika içeriğini (ağırlıkça %1,57) açıklayabilir. Buna ek olarak, çevredeki fliş için SMOW'a göre mil başına +13,3'lük oksijen izotopik değeri, Üst Jura-Alt Kretase'de çökeldiğini göstermektedir.


Eş zamanlı diferansiyel termal ve termogravimetrik (DTA/TGA) kızdırma eğrilerinde, ana termogravimetrik ağırlık kaybı 316,5 °C'de yaklaşık %52 ve toplam ağırlık kaybı 1400 °C'de yaklaşık %57'dir. Bu sonuçlar, Oltu taşının malzeme bileşenlerinin endüstriyel uygulamalarda aşırı ısınmaya karşı nispeten daha yüksek dirence sahip olduğunu göstermektedir.

Karbonlu Oltu taşı malzemelerinin, bazı yazarlar tarafından belirtildiği gibi fosil reçine veya fosilleşmiş ağaçtan türetilen karakehribar malzemesi olmadığı sonucuna varılmıştır. Turbostratik karbon malzemeler Dünyada endüstriyel kullanım için önemlidir. Oltu taşındaki  $sp^3$  bağlarının  $sp^2$  bağları ile bir arada bulunduğu tespit edilmiştir.  $sp^3$  bağları elmas kristalleri için çekirdeklenme alanları sağlayabilir ve elmas kaplamaların biriktirilmesinin erken aşamasında çekirdeklenme oranını artırabilir.

## ACKNOWLEDGEMENTS

The research was funded by Dokuz Eylül University BAP project numbered BAP.2012. KB.FEN.082. The authors is indebted to Berk Çakmakoglu for his technical support.

## ORCID

Cahit Helvacı  <https://orcid.org/0000-0002-8659-1141>

Murat Hatipoğlu  <https://orcid.org/0000-0002-4345-9052>

Danielle Passeri  <https://orcid.org/0000-0001-8189-1359>

Neşat Konak  <https://orcid.org/0009-0005-2874-9974> 

Eyyüp Hikmet Kınacı  <https://orcid.org/0000-0002-0267-7387>

## REFERENCES

- Bansal, R. C. & Donnet, J. B. (1993). *Carbon Black* (2<sup>nd</sup> ed.). In Donnet, J. B., Bansal, R.C. & Wang, M. J. (Eds.). Marcel Dekker, New York, 206–211.
- Bertrand, P. & Weng, L.T. (1999). Carbon black surface characterization by TOF-SIMS and XPS. *Rubber Chemistry & Technology*, 72(2), 384–398.
- Bilgin, Ö., Kalkan, E. & Dilmaç, M.K. (2011). Equipments used for production and processing of Oltu-stone. *The proceedings of 3<sup>rd</sup> Mining Machinery Symposium*, May 05-06, İzmir, Turkey, (in Turkish).
- Brown, I. D. & Altermatt, D. (1985). Bond valence parameters obtained from a systematic analysis of the inorganic crystal structure database. *Acta Crystallographica B*, 41, 244–247.
- Clague, A. D. H., Donnet, J. B., Wang, T. K. & Peng, J. C. M. (1999). A comparison of diesel engine soot with carbon black. *Carbon*, 37, 1553–1565.
- Çiftçi, E., Coşkun, S. & Yalçınalp, B. (2002). Oltu-stone-mineralogical and physical properties. 55<sup>th</sup> *Geological Congress of Turkey, Ankara, March 11–15. Proceedings Book of Abstracts* (pp. 34–35).
- Çiftçi, E., Yalçın, M. G., Yalçınalp, B., Kolaylı, H. (2004). Mineralogical and physical characterization of the Oltu-stone, a gemstone occurring around Oltu (Erzurum-Eastern Turkey). *International Congress on Applied Mineralogy (ICAM 2004)*, Águas de Lindoia, *Proceedings Book of Abstracts*, (pp. 537–539). Brazil, September 19–22.
- Donnet, J. B. (1994). Fifty years of research and progress on carbon black. *Carbon*, 32, 1305–1314.
- Franklin, R. E. (1950). Influence of the bonding electrons on the scattering of X-rays by carbon. *Nature*, 165, 4185–4193.
- Gruber, T. C., Zerda, T. W. & Gerspacher, M. (1993). Three-dimensional morphology of carbon black aggregates. *Carbon*, 31, 1209–1216.

- Gruber, T. C., Zerda, T. W. & Gerspacher, M. (1994). Raman studies of heat-treated carbon blacks. *Carbon*, 32, 1377-1384.
- Hatipoğlu, M., Ajo, D., Kibici, Y. & Passeri, D. (2012). Natural carbon black (Oltu-stone) from Turkey; a micro-Raman study. *Neues Jahrbuch für Mineralogie-Abhandlungen*, 189(1), 97-101.
- Hatipoğlu, M., Cesaro, S. N. & Ajo, D. (2014). Comparative Fourier transform infrared investigation of Oltu-stone (natural carbon black) and jet. *Spectroscopy Letters*, 47, 161-167.
- Hauptman, N., Vesel, A., Ivanovski, V. & Gunde, M. K. (2012). Electrical conductivity of Carbon Black pigments. *Dyes and Pigments*, 95, 1-7.
- Herrera-Alonso, M., Abdala, A.A., McAllister, M.J., Aksay, I.A. & Prud'homme, R. K., (2007). Intercalation and stitching of graphite oxide with diaminoalkanes. *Langmuir*, 23, 10644-10649.
- Hjelm, R.P., Wampler, W. & Gerspacher, M. (2000). The structure of carbon black and its associations in elastomer composites: a study using neutron scattering. *Kautschuk Gummi Kunststoffe*, 53, 592-599.
- Hunter, F. J., Mc Donnell, J. G., Pollard, A. M., Morris, C. R. & Rowlands, C. C. (1993). The Scientific identification of archaeological jet-like artefacts. *Archaeometry*, 35(1), 68-69.
- Jawhari, T., Roid, A. & Casado, J. (1995). Raman spectroscopic characterization of some commercially available carbon black materials. *Carbon*, 33, 1561-1565.
- Kalkan, E., Bilici, Ö. & Kolaylı, H. (2012). Evaluation of Turkish black amber: A case study of Oltu (Erzurum), NE Turkey. *International Journal of Physical Sciences*, 7, 2387-2397.
- Karayiğit, A. I., Kerey, İ. E., Bozkuş, C. (2002). Depositional environments of Oligo/Miocene coal-bearing strata and coal quality from the Oltu-Balkaya basin, northeastern Turkey. *Energy Sources*, 24, 653-665.
- Karayiğit, A. I. (2007). Origin and properties of Oltu gemstone coal. *Energy Sources Part A*, 29, 1279-1284.
- Kınacı, E. H. (2013). *Mineralogical and gemmological investigation and genesis of Oltu stone (Carbon Black)* [Unpublished Master's Thesis]. Dokuz Eylül University Graduate School of Natural and Applied Sciences.
- Koçyiğit, A., Öztürk, A., İnan, S. & Gürsoy, H. (1985). Tectonomorphology and mechanistic interpretation of the Karasu Basin (Erzurum). *Bulletin of Earth Sciences*, 2, 3-15.
- Kolodny, Y. & Epstein, S. (1976). Stable isotope geochemistry of deep-sea cherts. *Geochimica et Cosmochimica Acta*, 40, 1195-1209.
- Konak, N. ve Hakyemez, Y. (2008). 1/100.000 ölçekli Türkiye jeoloji haritaları Kars-G47 ve Kars-G48 Paftaları. MTA Report No: 104, (in Turkish).
- Lahaye, J. & Prado, G. (1981). *Particulate Carbon Formation during Combustion*. In Siegl, D. C. & Smith G.W. (Eds.). New York, Plenum Press, 35.
- Li, Z. Q., Lu, C. J., Xia, Z. P., Zhou, Y. & Luo, Z. (2007). X-ray diffraction patterns of graphite and turbostratic carbon. *Carbon*, 45, 1686-1695.
- Lin, J. H. (2002). Identification of the surface characteristics of carbon blacks by pyrolysis GC-MASS. *Carbon*, 40, 183-191.
- Probst, N. & Grivei, E. (2002). Structure and electrical properties of carbon black. *Carbon*, 40, 201-205.
- RRUFF. (2013). *Database of Raman spectroscopy, X-ray diffraction and chemistry of minerals* via <http://rruff.info/>.
- Smith, G. D. & Clark, R. J. H. (2004). Raman microscopy in archaeological science. *Journal of Archaeological Science*, 31, 1137-1160.
- Şengör, A. M. C., Görür, N. & Şaroğlu, F. (1985). Strike-slip faulting and related basin formation in zones of tectonic escape. Turkey as a case study. In *Strike-Slip Deformation, Basin Formation and Sedimentation*. SEMP Special Publications. 37, 227-264.
- Toprak, S. (2013). Petrographical properties of a semi-precious coaly stone, Oltu stone, from eastern Turkey. *International Journal of Coal Geology*, 120, 95-101.
- Tuinstra, F. & Koenig, J. L. (1970). Raman spectrum of graphite. *Journal of Chemical Physics*, 53, 1126-1132.
- Ungar, T., Gubicza, J., Ribarik, G., Pantea, C. & Waldek Zerda, T. (2002). Microstructure of carbon blacks determined by X-ray diffraction profile analysis. *Carbon*, 40, 929-937.
- Ungar, T., Gubicza, J., Tichy, G., Pantea, C. & Zerda, T. W. (2005). Size and shape of crystallites and internal stresses in carbon blacks. *Composites: Part A*, 36, 431-436.
- Wang, M. J. & Wolff, S. (1993). *Carbon Black* (2<sup>nd</sup> ed.). In Donnet, J. B., Bansal, R. C. & Wang, M. J. (Eds.), Marcel Dekker, New York, 229-246.
- Wang, A., Han, J., Guo, L., Yu, J., Zeng, P. (1994). Database of standard Raman spectra of minerals and related inorganic crystals. *Applied Spectroscopy*, 48, 959-968.
- Yu, Z.-M., Rogelet, T. & Flodström, S., A. (1993). Diamond growth on turbostratic carbon by hot filament chemical vapor deposition. *Journal of Applied Physics*, 74, 7235-7240.
- Zengin, Y. (1956). Oltu-taşı yatakları. *Bulletin of MTA (Turkey)*, 48, 148-149.
- Zerda, T. W., Xu, W., Zerda, A., Zhao, Y. & Von Dreele, R. B. (2000). High pressure Raman and neutron scattering study on structure of carbon black particles. *Carbon*, 38(3), 355-361.